

# Analysis of an iUPQC Operating as Interface for Microgrids with Power Angle Control

Matheus Montagner\*, Cassiano Rech\*\* and Marcelo Mezaroba\*

\* Santa Catarina State University - UDESC

Joinville - SC (e-mail: matheus.mtg60@gmail.com marcello.mezaroba@udesc.br ).

\*\* Federal University of Santa Maria – UFSM Santa Maria - RS (e-mail: cassiano.rech@gmail.com)

---

**Abstract:** The dual unified power quality conditioner (iUPQC) is an active filter that has been studied to be applied as utility interface in microgrid applications. It regulates the voltage of the microgrid side and controls the power flow between the grid and microgrid side. Besides that, ancillary functions to grid side have been proposed to extend its power quality compensation. This paper presents a detailed analytical and numerical analysis of the power flow of an iUPQC, which operates as an utility interface in microgrid applications with the extended function of STATCOM. It can compensate not only the disturbances at the load or microgrid side but also provides an RMS voltage regulation at the Point of Common Coupling (PCC), thus, providing reactive power to the grid. Moreover, the iUPQC power flow was evaluated considering the implementation of the power angle control (PAC), a technique used to share and equalize the power processed by each converter allowing the optimization of this conditioner. In addition, a test setup to validate this analysis was proposed and built. Therefore, this study can support the understanding of the power flow of the iUPQC operating as STATCOM, to share and optimize the available power in the iUPQC converters using PAC.

**Keywords:** iUPQC, microgrids, STATCOM, Power Angle Control (PAC), Power flow analysis.

---

## 1. INTRODUCTION

Distributed energy resources based on renewable energy source and the microgrid concept has been proposed as a solution to have electrical energy generation with less environment impact (Saeed et al. 2021) (Rezaei et al. 2021).

However, due to intermittence characteristic of renewable energy resources, microgrids topologies, control and operations strategies have been developed to ensure stable operation of microgrids (Espina et al. 2020).

In this sense, Utility Interfaces (UI) converters have been proposed for microgrid applications to make easier the controlling of the power system (Shubhra and Singh, 2020) (Tenti et al. 2014) (Machado et al. 2017). UI converter is connected between the grid and microgrid buses where the main function is to control the power flow between the buses (Shubhra and Singh, 2020) (Tenti et al. 2014). It makes easier the control of the power system once the control of a group of loads and generation is centered in the UI converter. In addition, it can be used to provide a regulated voltage in the microgrid side, improving the microgrid energy quality, and to provide ancillary functions to enhance the energy quality in the grid side (Shubhra and Singh, 2020) (Tenti et al. 2014) (Machado et al. 2017) (Khan et al. 2021).

The iUPQC originally is an active power filter (APF) and it is composed of a series active filter (srAPF) and a shunt active filter (shAPF) connected at the same DC bus in a back-to-back configuration. This configuration allows the conditioning of grid voltage and the load current simultaneously (Aredes and Fernandes, 2009) (Santos et al, 2014).

For the reason of iUPQC features, it is a converter topology that can be used as UI in microgrids, controlling the power flow between the grid and microgrid side, regulating the microgrid bus voltage and compensating the microgrid load disturbances (Paithankar and Zende, 2017) (França et al. 2015).

Besides that, the STATCOM functionality can be implemented in the iUPQC to auxiliary in regulation of the RMS voltage at the PCC by providing reactive power to the grid side (França et al. 2015). This functionality allows to optimize the use of the converter when there is available power to be processed in the converter, extending its functionalities and improving its viability. The operation of iUPQC as UI for microgrids and with the STATCOM functionality is called in this paper as multifunctional utility interface iUPQC (M-iUPQC).

In the iUPQC, the srAPF compensates the grid voltage disturbances while shAPF needs to compensate the load current disturbances. It means that under normal operation, with the PCC voltage around 1.0 pu, the power processed by shAPF is quite bigger than srAPF (Santos et al, 2014). This condition makes the srAPF underused, increases the conditioner losses and make difficult the modularization of the converters. This power unbalance issue is even more critical in an M-iUPQC because the shAPF needs to provide the reactive power to the microgrid and grid side while srAPF does not have power process (França et al. 2015).

To reduce the power unbalanced in the iUPQC, Fagundes (2016) and Fagundes (2021) proposed the Power Angle Control (PAC) technique. PAC consists of to impose a phase delay between the fundamental term of PCC voltage and load

voltage in such a way the allow the power sharing between the converters of iUPQC. However, there is a lack of studies providing either numerical or experimental evaluation of PAC technique considering iUPQC operating as STATCOM either for this conditioner operating as active filter or as UI in microgrids applications.

Therefore, this paper presents an analytical and numerical analysis of the power flow in the M-iUPQC with the PAC applied. The contribution of current study resides on to provide a numerical assessment of the power flow in a M-iUPQC. In addition, a test setup to validate experimentally the power flow analysis of a M-iUPQC was built and validated.

## 2. M-iUPQC POWER FLOW ANALYSIS

The main objective of this analysis is to obtain equations that describe the power flow between the converters of the M-iUPQC in function of  $\theta$ , which is the angle displacement of fundamental term of PCC voltage ( $v_{1pc}$ ) and fundamental term of current ( $i_{1pc}$ ), and  $\delta$ , which is the angle displacement between microgrid voltage ( $v_{1ul}$ ) and  $v_{1pc}$ , as are shown in Fig. 1.

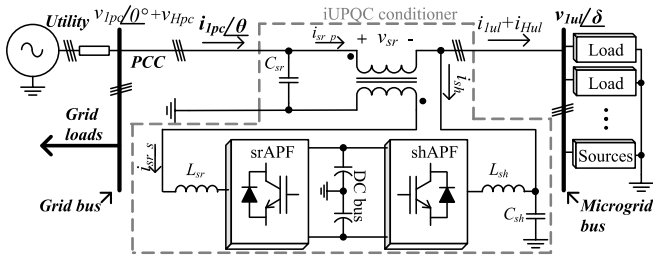


Fig. 1 Connection of a M-iUPQC between the grid and microgrid bus

### 2.1 Features of M-iUPQC and simplifications used in this analysis

In a closed-loop controlled iUPQC, the shAPF operates as a controlled voltage source and it imposes the load voltage to be sinusoidal and in phase with the PCC voltage ( $v_{1pc}$ ). In contrast, the srAPF operates as a controlled current source and maintains the PCC current ( $i_{1pc}$ ) balanced, with low distortion and in phase with  $v_{1pc}$ . Moreover, as stated by Santos et al. (2014), the iUPQC ideally does not have active power consumption and the amplitude of  $i_{1pc}$  is defined by the active power of the microgrid loads.

The M-iUPQC can provide reactive power to the grid side in order to auxiliary in the amplitude regulation of the PCC fundamental term voltage. This is done by controlling the fundamental quadrature term amplitude of the PCC current ( $i_{1pc}$ ) (França et al. 2015). The sum of the direct and quadrature components of the current in the PCC results in an equivalent current that has an angular displacement of  $\theta^\circ$  regarding to fundamental PCC voltage ( $v_{1pc}$ ). Consequently,  $i_{1pc}$  amplitude is not only defined by the loads active power of the microgrid loads as in the conventional iUPQC.

As previously stated, PAC technique consists of to impose a phase delay between microgrid and grid voltage. This phase displacement is represented by the  $\delta$  angle.

In addition, the power losses in the iUPQC as well as switching frequency harmonic components were ignored. Finally, the fundamental term of PCC voltage ( $v_{1pc}$ ) was defined as the reference voltage so that its phase angle is  $0^\circ$ .

To calculate the power flow of each converter, the concepts defined by IEEE 1459-2010 were adopted. This standard has definitions for measuring electric power quantities that were used in this paper as reference to evaluate each power term of the M-iUPQC converters that are fundamental active, reactive and apparent power, nonfundamental power and total apparent power. This methodology makes easy the understating of the effect of variation in each variable in the power flow in this conditioner. The polarities of voltages and currents are shown in Fig. 1.

### 2.2 Fundamental Power terms

To calculate the power in each converter, the amplitudes and angles of fundamental terms of current and voltage of srAPF and shAPF needed to be obtained.

The current of the  $C_{sr}$  capacitor was ignored because it is designed as a high-pass filter and, for grid frequency scale, this capacitor has a high impedance. Therefore, the srAPF current of M-iUPQC ( $i_{sr-p}$  in Fig. 1) was considered equal to PCC current ( $i_{1pc}$  in Fig. 1) and the amplitude of fundamental term of srAPF current can be obtained in function of microgrid active power, the fundamental term of PCC voltage and the angle  $\theta$ .

The amplitude and angle of srAPF voltage can be obtained by the difference between the fundamental term of PCC and the microgrid voltage.

The sum of the currents in node 1 was made to obtain the amplitude and angle of the shAPF current fundamental term. Lastly, the amplitude and angle of shAPF voltage are the microgrid voltage itself.

The fundamental power terms equations are given by (1) to (6).

$$P_{1srX}(\theta, \delta) = \frac{P_{ulT}}{V_{1pcT} \cdot \cos(\theta)} \cdot (V_{1pcX} \cdot \cos(\theta) - V_{1ul} \cdot \cos(\theta - \delta)) \quad (1)$$

$$Q_{srX}(\theta, \delta) = \frac{P_{ulT}}{V_{1pcT} \cdot \cos(\theta)} \cdot (V_{1ul} \sin(\theta - \delta) - V_{1pcX} \sin(\theta)) \quad (2)$$

$$S_{1srX}(\theta, \delta) = \sqrt{P_{1sr}(\theta, \delta)^2 + Q_{sr}(\theta, \delta)^2} \quad (3)$$

$$P_{1shX}(\theta, \delta) = \frac{P_{ulT} \cdot V_{1ul} \cdot \cos(\theta - \delta)}{V_{1pcT} \cdot \cos(\theta)} - V_{1ul} \cdot I_{1ulX} \cos(\varphi_{ulX}) \quad (4)$$

$$Q_{shX}(\theta, \delta) = V_{1ul} \cdot I_{1ulX} \sin(\varphi_{ulX}) - \frac{P_{ulT} \cdot V_{1ul} \sin(\theta - \delta)}{V_{1pcT} \cdot \cos(\theta)} \quad (5)$$

$$S_{1shX}(\theta, \delta) = \sqrt{P_{1sh}(\theta, \delta)^2 + Q_{sh}(\theta, \delta)^2} \quad (6)$$

Where suffix X indicates the respective phase,  $P_{ulT}$  is the total active power of the microgrid loads,  $V_{1pcX}$  is the fundamental PCC voltage in the respective phase,  $V_{1pcT}$  is sum of the amplitudes of the fundamental PCC voltages in phases A, B and C,  $V_{1ul}$  is the amplitude of microgrid voltage,  $I_{1ulX}$  and  $\varphi_{ulX}$  are the amplitude and angle of fundamental term of microgrid

load current in the respective phase where  $\varphi_{ulX}$  is the difference of the angle of microgrid voltage and current.

### 2.3 Nonfundamental and total power terms

In the M-iUPQC, the srAPF current and microgrid voltage, ideally, do not have harmonic distortion. Furthermore, the nonfundamental terms of microgrid load currents are compensated by shAPF. Therefore, the nonfundamental power term of shAPF ( $S_{Nsh}$ ) is given by (7).

$$S_{Nsh}(\theta, \delta) = V_{1ulX} \cdot I_{1ulX} \cdot THD_{iulX} \quad (7)$$

Where  $THD_{iulX}$  is total harmonic distortion of the current in the respective phase.

The nonfundamental power of srAPF ( $S_{Nsr}$ ) is shown in (8) and is given by the product of nonfundamental PCC voltage and srAPF current.

$$S_{Nsr}(\theta, \delta) = V_{1ulX} \cdot THD_{vpCX} \cdot \frac{P_{ulr}}{V_{1pCr} \cdot \cos(\theta)} \quad (8)$$

Where  $THD_{vpCX}$  is total harmonic distortion of the PCC voltage in the respective phase.

Finally, (9) and (10) give the total apparent power srAPF ( $S_{sr}$ ) and shAPF ( $S_{sh}$ ).

$$S_{sr}(\theta, \delta) = \sqrt{S_{1sr}(\theta, \delta)^2 + S_{Nsr}(\theta, \delta)^2} \quad (9)$$

$$S_{sh}(\theta, \delta) = \sqrt{S_{1sh}(\theta, \delta)^2 + S_{Nsh}(\theta, \delta)^2} \quad (10)$$

With these equations, it is possible to evaluate the power flow of each phase in the M-iUPQC using PAC.

## 3. SIMULATIONS AND EQUATIONS VALIDATION

To validate the previous mathematical analysis, numerical simulations using the software PSIM 9.0 were performed. The simulated system consists of an M-iUPQC operating as a microgrid interface converter, as shown in Figure 1, where the grid is providing active power to the microgrid loads. The design of the power elements and control strategy of the conditioner was made as is presented by Santos et al. (2014). The microgrid was modeled as a load set composed by a linear RL, a three-phase rectifier with capacitive filter and a RL load supplied by a single-phase full-wave rectifier. A balanced microgrid loads and PCC voltages scenario was evaluated.

The simulations were performed using the following specifications:

- Nominal apparent power of iUPQC: 2.5 kVA.
- Microgrid bus line voltage: 220 V.
- Fundamental PCC line voltage: 220 V.
- PCC voltage total harmonic distortion (THD): 11.6%.
- Total apparent power of microgrid loads: 1.71 kVA.
- Fundamental apparent power of microgrid loads: 1.68 kVA.
- Fundamental power factor of microgrid: 0.89, lag.
- THD of microgrid load current: 20%.

The PCC voltage and microgrid current signals is shown in Fig. .

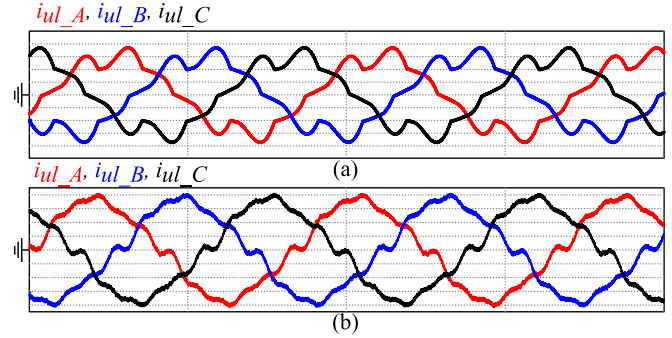


Fig. 2 (a) Microgrid load current (2 A/div, 10 ms/div) and (b) PCC voltage (50 V/div and 10 ms/div) signal of balanced scenario.

The simulations were performed varying  $\theta$  and  $\delta$  angles in a range of  $0^\circ$ ,  $\pm 20^\circ$  and  $40^\circ$ . The single phase calculated and simulated results of fundamental active, reactive and apparent power terms of srAPF shared and shAPF are shown in Fig.3 (a) to Fig. 3(e), respectively, where the marked points are the simulated results and the line graphs are the calculated results. As are shown in Fig. 3, the simulated and calculated results of fundamental terms converged to the same values for all simulations performed, validating the equations obtained in this analysis.

Additionally, with  $\theta$  e  $\delta$  in  $0^\circ$ , the reactive power of srAPF (Fig. 3(b)) is around zero while the reactive power of shAPF (Fig. 3(d)) is equal to the reactive power of microgrid loads. It is caused because the fundamental PCC voltage is equal to the load voltage and there is no voltage across srAPF transformer.

Consequently, there is not power in srAPF. However, in the M-iUPQC, all current from grid to microgrid side flow by srAPF. For this reason, srAPF has power losses in function of the current however it does not compensate the load disturbances. Keeping  $\delta$  equal to  $0^\circ$  and for positive  $\theta$  angles, iUPQC is providing reactive power to the grid. However, the srAPF voltage is kept in 0 V and the shAPF needs to supply the reactive for grid and load, increasing shAPF power as previously stated. It increases the unbalanced power compensated by each converter.

Changing the angle  $\delta$ , a voltage across srAPF transformer is imposed. Consequently, the srAPF starts to have power processing. For positive  $\delta$  angle, srAPF also supply reactive power then shAPF supply less power, decreasing the power that shAPF need to compensate. Even though, for  $\delta$  different of  $0^\circ$ , active power circulates between srAPF and shAPF (Fig. 3(a) and Fig. 3(d)), the fundamental apparent power, of shAPF decreases considerably, as show in Fig. 3(c) and 3(f). For this reason, PAC is efficient to balance the power compensate by each converter and for optimizing iUPQC, compensating more power with the same hardware, increases the efficiency because the current in shAPF reduces and make modular projects easier as soon as the power processed by each converter can be balanced.

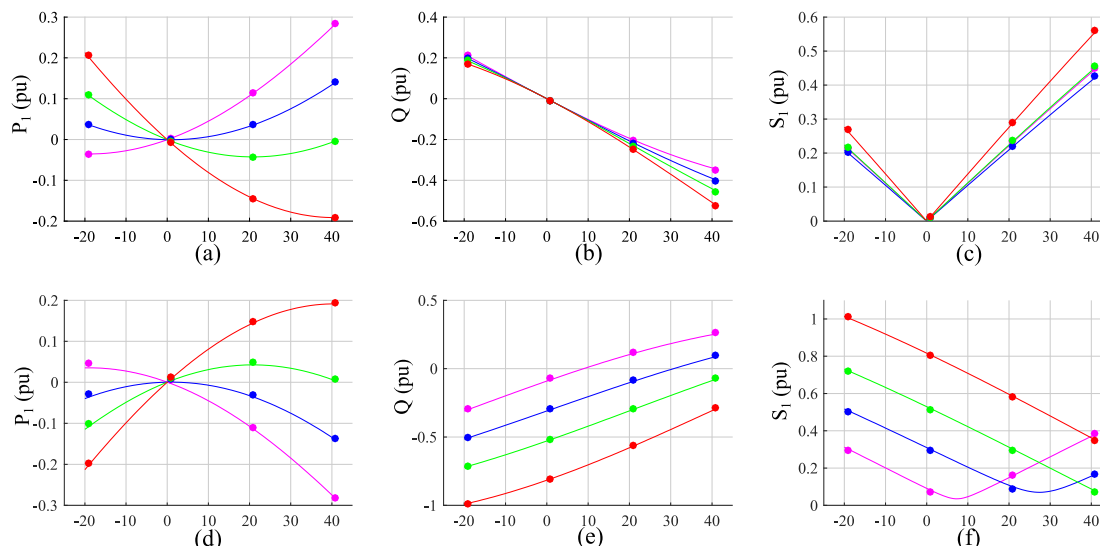


Fig. 3 Calculated and simulated results of fundamental terms in balanced scenario. (a) fundamental term of active power of srAPF, (b) fundamental term of reactive power of srAPF, (c) fundamental term of apparent power of srAPF, (d) fundamental term of active power of shAPF, (e) fundamental term of reactive power of shAPF, (f) fundamental term of apparent power of shAPF.

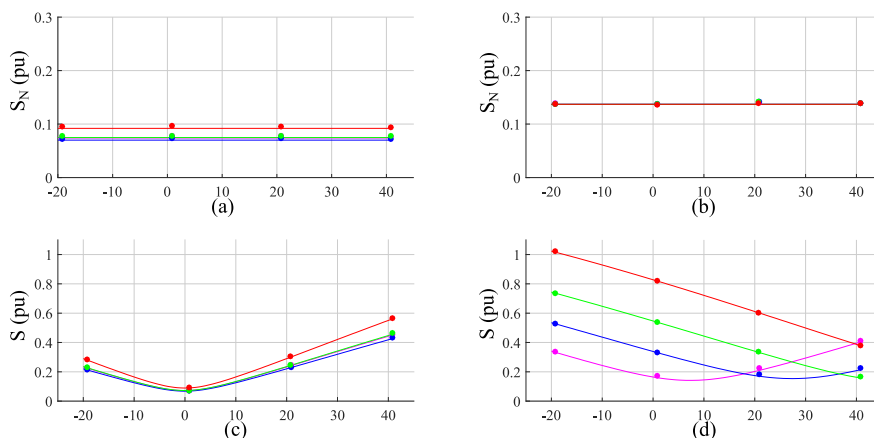


Fig. 4 Calculated and simulated results of nonfundamental and total apparent power terms of balanced scenario. (a) nonfundamental power term of srAPF, (b) nonfundamental power term of shAPF, (c) total apparent power of srAPF, (d) total apparent power of shAPF.

For the nonfundamental power terms of srAPF and shAPF, as shown in Fig. 4(a) and Fig. 4(b), respectively, there is a small difference between simulated and calculated results. It is caused by the harmonics of current and voltage in the switching frequency, which was not considered in the equations developed. Anyway, this noted difference did not affect significantly total apparent power of srAPF and shAPF, as are shown Fig. 4(c) and Fig. 4(d), respectively.

Besides that, the  $\delta$  variation does not imply in nonfundamental power sharing between the srAPF and shAFP. The srAPF compensates all the harmonic terms of PCC voltage and the shAPF, compensates all harmonic terms of load current. It means that using PAC is not possible to share the power nonfundamental power terms between the converters of iUPQC. In applications where the load harmonic content be very high, the PAC technique may be not much useful to balance the power of iUPQC converters. Anyway, in this scenario and considering the advantages of balance the powers

of iUPQC converters, the PAC technique can be applied to balance the power between the converters of iUPQC

#### 4. EXPERIMENTAL TEST SETUP

To validate experimentally the analysis and the equations obtained in this paper, a test setup of a M-iUPQC was proposed, assembled and validated. The main goal of this test setup is to allow the validation of the power flow analysis of a M-iUPQC proposed in this paper. Therefore, in the proposed test setup, the  $\delta$  and  $\theta$  angles can be set by the user. Moreover, to allow the evaluation of the impact of other variables in the power flow of the M-iUPQC, rather than  $\delta$  and  $\theta$ , sag and swells can be controlled as soon as the load set can be selected to change the microgrid's loads characteristics.

The built M-iUQPC has the same specifications and values used in the converter simulated to validate the equations, in the previous section. The M-iUQPC assembled is shown in the Fig. 5.

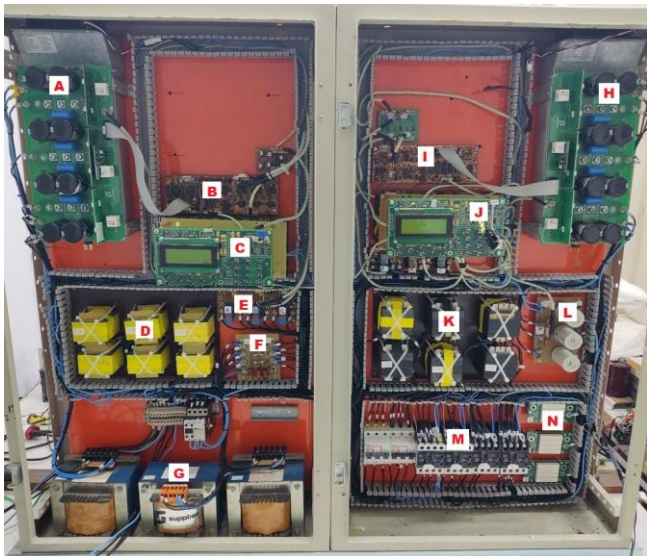


Fig. 5 M-iUPQC built.

The identified parts A to G shown in the Fig. 5 are related to srAPF which are (A) inverter module, (B) control board, (C) reference signal generator and human machine interface (HMI), (D) inductors, (E) current sensors, (F) high frequency capacitors and (G) coupling transformers. The parts H to L are related to shAPF which are (H) inverter module, (I) control board, (J) reference signal generator and HMI, (K) inductors and (L) high frequency capacitors. The parts M and N are, respectively, the contactors and resistors used in the precharge of the DC link capacitors. At the end, the identified parts O are the circuit brakes to protect against high currents at the input and output of the converter.

The experimental tests were performed in a scenario where the grid is providing active power to the microgrid, as were made in the simulations performed. A balanced load set were made using passive components as resistors and inductors and nonlinear devices as three-phase rectifiers.

The M-iUPQC was fed by the lab grid through a three-phase variable transformer that allow the simulation of sag and swells. The output of the variable transformer was defined as the PCC of the system. To introduce harmonic distortions in the PCC voltage, a nonlinear load made by a three-phase rectifier with a capacitor filter and resistive load were used. Finally, the control of the  $\theta$  and  $\delta$  angles is made by the HMI of srAPF and shAPF. This HMIs can generate a sinusoidal reference signal with a selectable phase regarding the PCC voltage. The HMIs generated signals is used as reference signal to the srAPF current control and shAPF voltage control. To keep the same phase between the PCC voltage and the reference signal generated by the HMIs, a PLL strategy was adopted.

Firstly, the  $\delta$  and  $\theta$  angles were set to  $0^\circ$ . The microgrid voltage and current of the three phases were captured. The waveforms captured are shown in the Fig. 6.

Using power analyzers, PCC voltage and microgrid voltage current and active power were measured. The measured values are shown in the Table 1, where is shown that the microgrid voltage is balanced and with very low harmonic content.

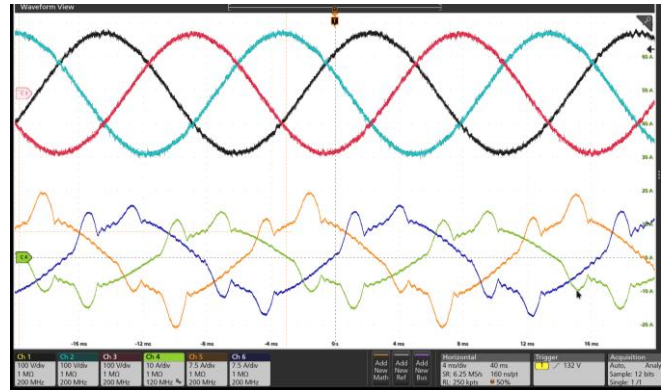
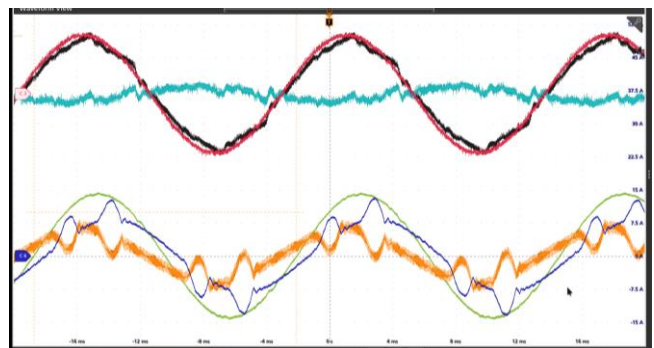


Fig. 6 Measured waveforms of microgrid voltage (CH1 phase A, CH2 phase B, CH3 phase C, 100 V/div) and current CH4 (10 A/div) phase A, CH5 phase B, CH6 phase C, (7,5 A/div).

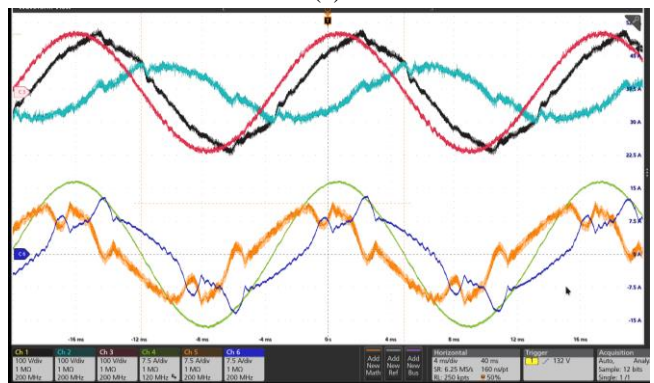
Table 1. Measured PCC voltages and microgrid loads

Parameter	phase		
	A	B	C
RMS microgrid voltage (V)	126.5	126.9	126.3
THD of microgrid voltage (%)	0.92	0.60	0.58
RMS microgrid current (A)	7.22	7.56	7.50
THD of microgrid current (%)	20.7	21.9	22.1
Microgrid active power (W)	751	799	762
PCC RMS voltage (V)	115.9	114.3	114.7
THD of PCC voltage (%)	6.3	5.7	6.0

To validate the  $\delta$  and  $\theta$  control, a test with  $\delta$  and  $\theta$  set to  $0^\circ$  and  $-20^\circ$ , respectively, and another test with both  $\delta$  and  $\theta$  set to  $20^\circ$ . The waveforms captured are shown in Fig. 7.



(a)



(b)

Fig. 7 Voltage waveforms (100 V/div) of PCC (CH1), srAPF (CH2) and microgrid (CH3), and current waveforms of PCC (CH4), shAPF (CH5) and microgrid (CH6). Angles setup (a)  $\delta = 0^\circ$ ,  $\theta = -20^\circ$  and (b)  $\delta = \theta = 20^\circ$ .

Where the channels 1 to 3 are the measured voltage of PCC, srAPF and microgrid voltage, respectively. The channels 4 to 6 are the current of PCC, shAPF and microgrid, respectively. All measured values of Fig.7 were measured in the phase A of the system.

In the Fig. 7 (a) is shown that the PCC current is lagged related to PCC voltage which means that the M-iUPQC is providing reactive inductive power to the grid side. In the Fig. 7 (b) is shown that PCC voltage is lagged regarding the PCC current which means that the M-iUPQC is providing reactive capacitive power to the grid side. It demonstrates that the  $\theta$  angles control is effective and the controllers of the M-iUPQC are following the imposed reference.

Besides that, in the Fig. 6(b) is demonstrated that the microgrid voltage is lagged regarding PCC voltage, which also demonstrates the effectiveness of the  $\delta$  control.

Given these facts, the test setup was validated and it could be used to experimentally validate the power flow analysis of a M-iUPQC proposed in this paper.

## 5. CONCLUSIONS

In this paper, the power flow in the M-iUPQC using PAC was evaluated through analytical and numerical simulation. It was demonstrated that PAC is efficient to control and balance of the power processed by each converter of M-iUPQC even with the variation of  $\theta$  angle. In addition, with the balancing of the power process by each converter, it was demonstrated that in the scenario evaluated the total power that a M-iUPQC can process increases because the use of srAPF is optimized, reducing the power processed by shAPF. This feature is important to allow M-iUPQC to provide more power reactive power to grid when it is operating as STATCOM.

Besides that, a test setup to experimentally validate the power flow analysis of a M-iUPQC was built and validated through preliminary experimental tests. The next steps, the authors are considering the experimental evaluation using the current proposed setup. In addition, the authors are considering the development of a control strategy of PAC with the goal to optimize the use of the converters of a M-iUPQC.

## ACKNOWLEDGMENT

This work was developed with the support of Programa Nacional de Cooperação Acadêmica da Coordenação de Aperfeiçoamento de Pessoal de Nível Superior CAPES/Brazil. This research was funded by Conselho Nacional de Desenvolvimento Científico e Tecnológico (CNPq), grant number 465640/2014-1; Coordenação de Aperfeiçoamento de Pessoal de Nível Superior (CAPES), grant number 23038.000776/2017-54; Fundação de Amparo à Pesquisa do Estado do Rio Grande do Sul (FAPERGS), grant number 17/2551-0000517-1; Fundação de Amparo à Pesquisa e Inovação do Estado de Santa Catarina (FAPESC), grant number 2017TR656;

## REFERENCES

Saeed, M. H., Fangzong, W., Kalwar, B. A., Iqbal, S. (2021) "A Review on Microgrids' Challenges & Perspectives," in

- IEEE Access, vol. 9, 166502-166517, doi: 10.1109/ACCESS.2021.3135083.
- Espina, E., Llanos, J., Burgos-Mellado, C., Cárdenas-Dobson, R., Martínez-Gómez, M., and Sáez, D. (2020). "Distributed Control Strategies for Microgrids: An Overview," in *IEEE Access*, vol. 8, 193412-193448, doi: 10.1109/ACCESS.2020.3032378.
- Shubhra, Singh, B. (2020). "Solar PV Generation Based Microgrid Control Interfaced to Utility Grid," in *21st National Power Systems Conference (NPSC)*, 1-6, doi: 10.1109/NPSC49263.2020.9331928.
- Tenti, P., Caldognetto, T., Buso, S., Costabeber A. (2014). "Control of utility interfaces in low voltage microgrids. In *2014 IEEE 5th International Symposium on Power Electronics for Distributed Generation Systems (PEDG)*, 2014, pp. 1-8, doi: 10.1109/PEDG.2014.6878674.
- Machado, A. A. P., Brandao, D. I., Pires, I. A., Filho, B. d. J. C. (2017). Fault-tolerant Utility Interface power converter for low-voltage microgrids. In *IEEE 8th International Symposium on Power Electronics for Distributed Generation Systems (PEDG)*, 1-5. doi: 10.1109/PEDG.2017.7972469.
- Khan, I., Vijay, A. S., Doolla, S. (2021). Nonlinear Load Harmonic Mitigation Strategies in Microgrids: State of the Art. In *IEEE Systems Journal*, 1-13. doi: 10.1109/JSYST.2021.3130612.
- Aredes, M., Fernandes, R. M. (2009). A dual topology of Unified Power Quality Conditioner: The iUPQC. In *13th European Conference on Power Electronics and Applications*, pp. 1-10.
- Santos, R. J. M., Cunha, J. C., Mezaroba, M. (2014). A Simplified Control Technique for a Dual Unified Power Quality Conditioner. In *IEEE Transactions on Industrial Electronics*, 61 (11), 5851-5860. doi: 10.1109/TIE.2014.2314055.
- Paithankar, S., Zende, R. (2017). Comparison between UPQC, iUPQC and improved iUPQC. In *Third International Conference on Sensing, Signal Processing and Security (ICSSS)*, 61-64, doi: 10.1109/SSPS.2017.8071565.
- França, B. W., Silva, L. F., Aredes, M. A. (2015). An Improved iUPQC Controller to Provide Additional Grid-Voltage Regulation as a STATCOM. In *IEEE Transactions on Industrial Electronics*, 62 (3), 1345-1352. doi: 10.1109/TIE.2014.2345328.
- Fagundes, S.M., Cardoso, F.L., Stangler, E.V., Neves, F.A.S., Mezaroba, M. (2021). A detailed power flow analysis of the dual unified power quality conditioner (iUPQC) using power angle control (PAC). In *Electric Power Systems Research*, 192. doi: 10.1016/j.epsr.2020.106933.
- Fagundes, S. M., Mezaroba, M. (2016). Reactive power flow control of a Dual Unified Power Quality Conditioner. In *IECON 2016 - 42nd Annual Conference of the IEEE Industrial Electronics Society*, 1156-1161. doi: 10.1109/IECON.2016.7793770.
- IEEE Standard Definitions for the Measurement of Electric Power Quantities Under Sinusoidal, Nonsinusoidal, Balanced, or Unbalanced Conditions (2010). In *IEEE Std 1459-2010 (Revision of IEEE Std 1459-2000)*, vol., no., pp.1-50, 19. doi: 10.1109/IEEESTD.2010.5439063.